

# Imaging the 1997 Marseille fire

I. Piccolini, O. Arino, A. Arnaud & J-M. Rosaz

ESA/ESRIN, Directorate of Application, Remote Sensing Exploitation Department  
CP 64, Via Galileo Galilei, 00044 Frascati, Italy

On 26 July 1997, a large fire spread in the hills close to Marseilles. A collection of satellite images were processed in order to demonstrate the capabilities and the limitations of the current remote sensing instruments (and data) for fire detection, fire monitoring and damage assessment. The first results were presented at the Eurisy Conference in Morocco in September 1997 on Application of Space Techniques for Hazard Management in the Mediterranean.

The low-resolution instruments (AVHRR and ATSR) provided a limited detection and monitoring capability due to the acquisition frequency and to a lower extent, the spatial resolution. The repeat cycle of both ERS and NOAA satellites was a limiting factor. The high-resolution ERS SAR and Landsat TM instruments provided precise identification of the extent of the damage. The Marseille fire was used as a test case in order to analyse the precision of the ATSR radiometry sequence of the event in order to build on a burned-surface estimation algorithm.

## Detection and monitoring

The revisit frequency of both the AVHRR and the ATSR theoretically allows the acquisition of data 4 to 6 times per 24 hours over the same area in Europe. Morning and afternoon NOAA satellite passes provide four acquisitions per day with a 3000-km swath. Night-time AVHRR data are not systematically acquired by ground stations without a meteorological mandate. Figure 1 shows all daytime acquisitions of the AVHRR.

At European latitude, the 500-km ATSR swath only allows coverage of a specific European area every 3 days (during daytime: descending pass) and the same coverage (during nighttime: ascending pass).

In Figure 2, a large smoke plume is clearly visible on both AVHRR and ATSR images the day of the fire. In the AVHRR images, the Arino & Melinotte fire detection algorithm was applied and pixels with hot spots were evident. No active fire detection was possible with the ATSR daytime data due to an early saturation of the 3.7 channel (Fig. 5), but it is visible on the 1.6 micron channel due, certainly, to the high (fire) temperature [Dozier 1981].

## Damage assessment

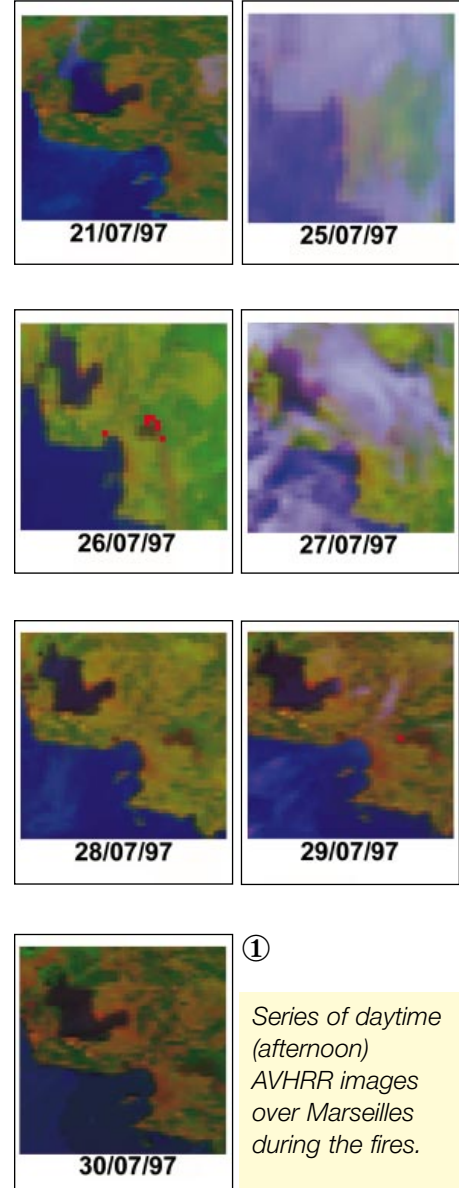
The precise extent of the burned area can be derived from the high-resolution

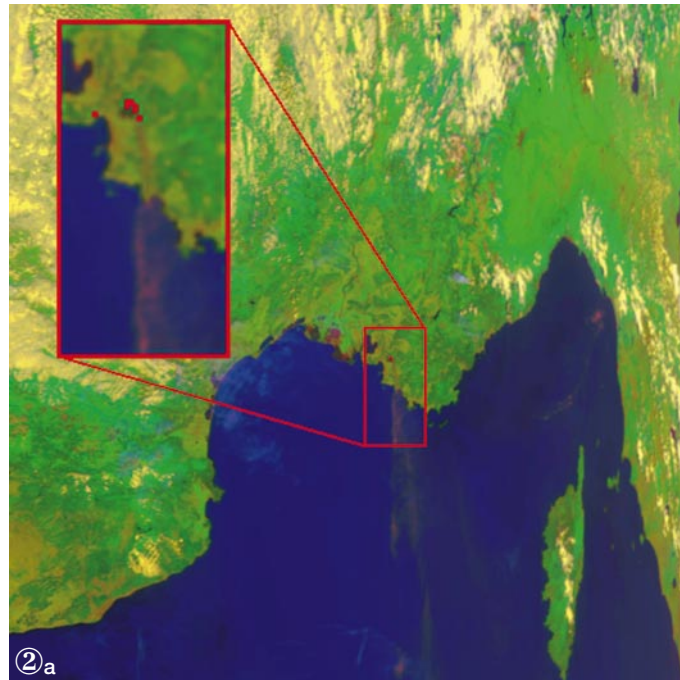
optical images (e.g. Landsat TM). Correcting for atmospheric effects [Arino *et al.* 1987] increases the contrast. More accurate identification was performed using band 4, which is shown on Figure 4. The precise extent can also be derived from SAR data, which were not required for the Marseille case but are necessary when dealing with tropical heavily-clouded regions (Fig. 3) [Antikidis *et al.* 1998].

## Global biomass burning atlas

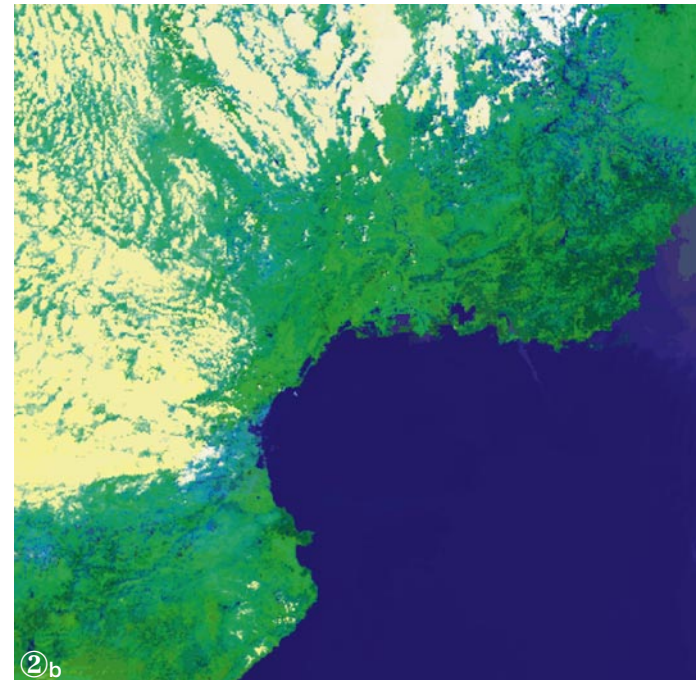
Biomass burning atlases are required by the scientific community [Andreae 1991]. The development of a global burned surface algorithm, which at the moment does not exist, is ongoing for AVHRR, vegetation, MODIS and ATSR. Regional attempts with either AVHRR or ATSR [Eva *et al.* 1995 & Pereira 1996] produced interesting results. Imaging the Marseille fire provided us with the opportunity to fully analyse the radiometric behaviour of the ATSR-2 channels (both nadir and forward, and visible and infrared) (Fig. 5)

This test-bed derived simple radiometric rules. Figure 6 is an illustration of one of these simple rules. Applying this to ATSR data, one can obtain significant results for comparison with the TM image (Fig. 7). The temporal co-registration of ATSR images has been analysed (Fig. 8) to increase the number of potential radiometric rules by adding temporal behaviour rules.





Subsample of AVHRR quicklook image acquired on 26 July 1997.



ATSR quick-look image acquired on 26 July 1997.

### Figure description

Figure 1 shows the situation for seven different days, three before, one during and three after the occurrence of the fires with AVHRR images. In particular, for 26 & 29 July 1997, it is possible to see the pixels where active fires were detected by the Arino & Melinotte algorithms. The main problem that arises from this monitoring is the daily variation of the image contrast. The AVHRR swath (3000 km) leads to a large number of different observation angles for the same zone at different days. These radiometric changes are attributed mainly to the bi-directional effects of the surfaces and its coupling with the atmospheric effects. Another problem occurs in this large swath situation: the different effective ground resolution of pixels observed at the same angular field of view does not allow a correct estimation of the burned area when using temporal co-registration of the images.

In Figure 2a, we can see the Marseille area and the pixels with active fire estimated by an algorithm based on both thermal and visible channels [Arino & Melinotte 1985]. One can notice the presence of 2 hot spot sites, one close

to Marseille and the other situated on the Estaque mountains. Figure 2b shows a colour composite of quick-look based on 0.67 micron (red), 0.87 micron (green) and inverted 11 micron (blue). The smoke plumes from the Marseille fires are clearly visible in a SSE direction.

Figure 3 is composed of two SAR images, one acquired on 24 May, before the fire, the other on 2 August, after the fire. In order to detect the burned surfaces, a multi-temporal image was created, combining these two acquisitions. The green channel has been assigned to the average intensity of both images; the red channel corresponds to the intensity difference; the phase coherence computed from the two complex images has been assigned to the blue channel.

The fire creates a drastic change in humidity and roughness of the surface. Therefore, it contributes to a strong intensity change in this specific case of the Mediterranean forest. This intensity change has not been observed for other types of forests such as the rain forest [Antikidis *et al.* 1998, in this issue]. In order to enforce this charac-

terisation of surface change, the interferometric coherence has been added. The coherence, though low for forest, decreases to zero when computed between the forest and the burned area. As a consequence, burned surfaces with high-intensity changes, standard average intensity and low coherence appear in orange. This clear characterisation from the rest of the image, defines the position and extent of burned surfaces to the northeast of Marseille, and of a smaller fire on the other side of the bay. The city appears in cyan (high intensity and high coherence values). The processing was performed using the Diaphason software from CNES.

The Landsat scene in Figure 4 was acquired at Fucino (I) on 3 August. This is a system-corrected product which takes atmospheric effects into account in order to increase contrast [Arino *et al.* 1997]. A TM atmospheric product is calibrated then corrected for gas absorption, Rayleigh and aerosol scattering. The products provide reflectance in the six visible and near infrared channels. The image presented is channel 4 without any processing other than re-scaling. This channel (760–900 nm)

is very sensitive to vegetation response because it is located after the red edge. The reflectance in this channel for the same non-burned vegetation has twice the reflectance over burned areas. This is due to the disappearance of the vegetation which used to have a high reflectance value in this channel.

Channel 1 reflectance after the fire was found to have doubled, but the discrimination with other land cover was difficult to determine. Reflectance in channel 7 was tripled by the fire and should, therefore, offer the best discrimination potential, but it was difficult to separate urban areas from burned surface. The temperature retrieved in channel 6 provides a clear evidence of the burned area due to still-warm burn scars and, also, to a different radiative behaviour of the surface.

Figure 5a is a sub-sample of 50 x 30 km derived from the images observed by all the different channels of the ATSR-2 sensor for three days of the fire zone. From an analysis of these, we can see that the active fire leads to an increase in brightness temperature in both the 11- and 12-micron channels. Some fires are large enough to saturate these channels and appear in black. Other information contained in the thermal channels is the increase in the surface temperature for the burned surfaces appearing in the 29 July images. Since the 3.7 micron has a low brightness temperature of saturation (311 K), this channel appears saturated for

many pixels. In the 1.6 micron image, it is also possible to see the active fires because the high temperature of the fire leads to a high energy emission at this wavelength. The spectral normal reflectance of vegetation is high in the near-infrared channel. When the vegetation is burned this reflectance decreases to a low level (more or less like the water reflectance).

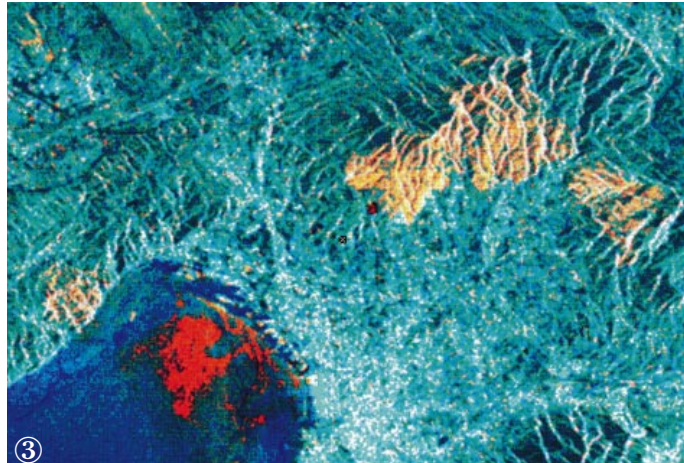
In these images, at 0.87 micron, it is possible to note the occurrence of burned surfaces and to monitor their extension. In the 26 July image it is possible to see a line of low reflectance near the burned surface. This is the shadow of the smoke plumes that we can see better in the visible channels because the scattering is higher at small wavelength, in the visible channels (0.55 and 0.67 micron). An estimation of the direction of the smoke plumes is therefore possible. Moreover, in these channels, the different atmospheric situation is visible between the first and the last day and presents an increase in terms of atmospheric haze leading to a global decrease of the image contrast.

In the forward-view images (Fig. 5b), we can more or less see the same characteristics as the nadir images, with the difference that the contrast is lower because of a long path of radiation along the atmosphere, and the pixel resolution has been altered by the angular observation of 55°. In the IR channels, it is always possible to note

the active fires as well as a little increase in the burned surfaces, but the channels do not saturate. The only relevant information that we can extract from the forward-view images is derived from the 3.7 micron channel. This channel is saturated only in the zone of burned surfaces of active fire. This allows a rapid estimation of the extent of the burned area. In the 1.6 channel it is possible to see the pixels with active fire and in the 0.87 micron channel the low reflectance for the burned surfaces. Due to the long atmospheric path, the contrast decreases within the visible channels, allowing a better perception of the smoke plumes, but the increase in atmospheric haze for the third day led to images with little information.

The burned surfaces (Fig. 6) present an increase of 7- 8°C for a decrease of 20% reflectance in the NIR because of the absence of vegetation. For these reasons, the pixels of burned surfaces in the scatterplot between 0.87 micron and 11 micron channel appear in the upper left zone (off the cluster of normal vegetation pixel or water condition). The variation of the atmospheric daily situation can change the contribution to the TOA reflectance. In this case, all the pixels mapped in the scatterplot are shifted to the lower right side (see the difference between the scatterplots of the 23 & 29 July images). Only a dynamic algorithm leads to the correct estimation of the pixels that present the characteristics of burned surfaces. The

ERS-2-SAR composite image of the Marseille area.

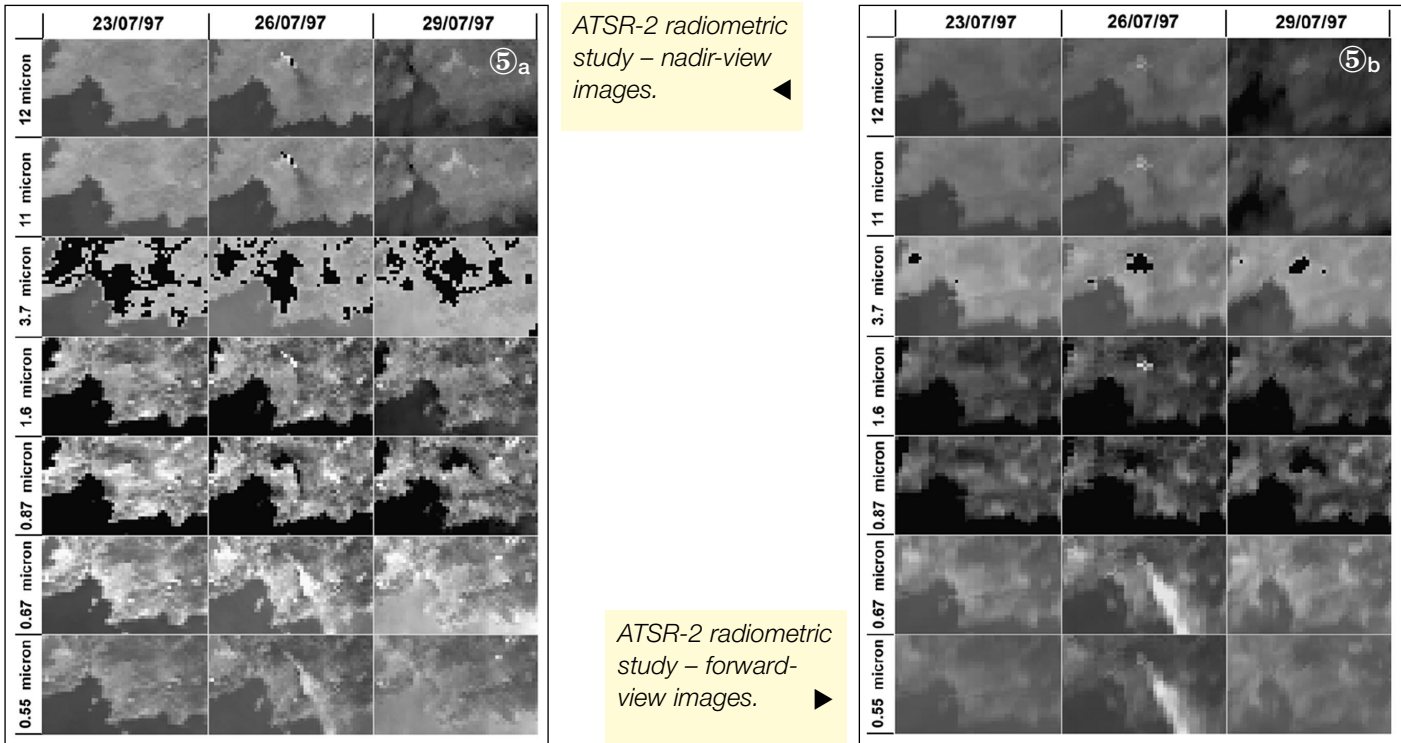


③

Landsat band 4 (atmospheric correction).



④



black line is the regression line for each scatterplot that varies daily in position. A threshold (red line) is linked to the regression line and will shift in position according to the daily condition leading to a correct choice of burned surface pixels that are above this 'dynamic' threshold.

In Figure 7 we can see the reflectance derived from ATSR-2 at 0.87 micron during three days of observation. The yellow pixels are burned surfaces estimated by the dynamic algorithm. From a comparison with high-resolution data (Landsat) of the burned surface we can see the high level of confidence of this estimation. The second image (26 July)

shows a dark line below the burned surface, this is the effect of the smoke plume's shadow, which is not correctly estimated to be burned surface as expected. This method, when coupled with a Land Cover Map, leads to an estimate of the total amount of biomass lost, of the gaseous material and of aerosol particles released [Andreae 1991].

In order to make a temporal analysis with ATSR-2 data over the same zone, it is necessary to be sure that the pixels are superimposed. The ATSR-2 images (GBT: Gridded Brightness Temperature) have latitude/longitude values for each pixel that are estimated during the

process of remapping the conical scans in raster images. Figure 8 shows the position of each pixel taken from the three days' images. We can see that there is shift and rotation between the three grids of pixels, which does not allow a pixel-based temporal analysis before remapping. Moreover, the GBT images have an x/y offset value (fraction of 1 km) which restores the accuracy of the original grid-mapping process.

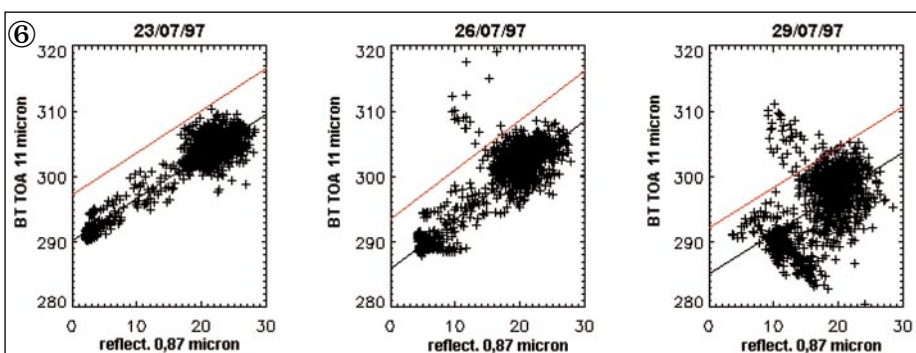
However, using this data for remapping leads to the difficulty of working without raster images. The other possible solution is to relocate the sub-image by a cross-correlation between successive observations. In this case, we can obtain a series of images which can, more or less, be superimposed, and which allow a pixel-based temporal analysis.

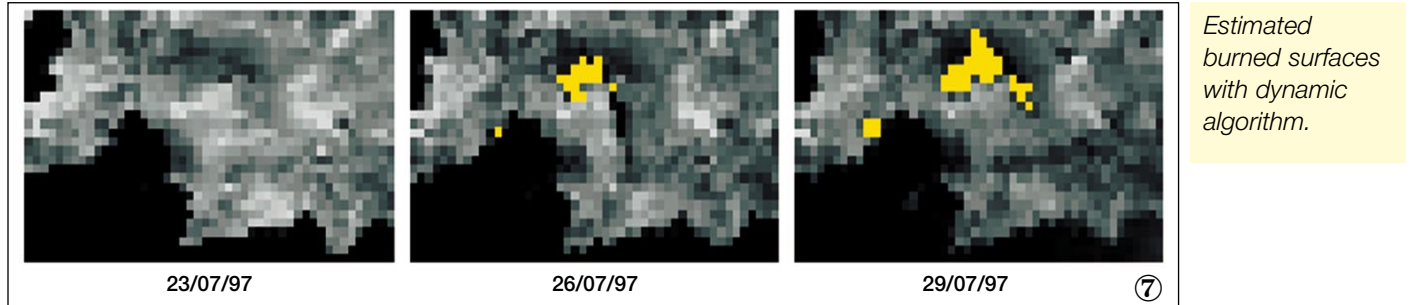
## Conclusion

The extensive imaging of the Marseille fire showed that:

- the detection and monitoring capacity of the actual low bit-rate sensor is somewhat limited by the quick saturation of the 3.7 micron channel (320 K for AVHRR and 311 K for ATSR), because these sensors were originally conceived to provide the maximum radiometric dynamic of

### Preliminary dynamic algorithm for burned-surface estimation with ATSR-2 data.





ocean temperatures. The spatial and temporal resolution is not sufficient in regards to European firefighters requirements ( $10^2$  m and 10 min from the outbreak of the fire) [Martin Rico 1998];

- current high-resolution satellites are perfectly suited for fire damage assessment;
- ATSR radiometry analysis indicated ATSR's ability to map the burned surfaces within the Mediterranean area. This needs to be extended to other coverage types.

### Acknowledgements

We would like to express our appreciation to F. Cattaneo and P. Goryl in support of data ordering and processing, and M. Gorman for his essential inputs and for reviewing the paper.

### References

Andreae M: Biomass burning: Its history, use and distribution and its impact on environmental quality and global climate: *Global biomass burning, atmospheric, climatic & biospheric implication*, Ed. J.S. Levine, 3-21, 1991.

Antikidis E, O Arino, H Laur & A Arnaud: Deforestation evaluation by synergistic use of ERS SAR coherence and ATSR hot spots: The Indonesian fire event of 1997, *EOQ*, 59, 1998.

Arino O & J-M Melinotte: Fire Index Atlas, *EOQ*, 50, Dec. 1995.

Arino O, E Vermote & V Spaventa: Operational atmospheric correction of Landsat TM imagery. *EOQ*, 56-57, Dec. 1997.

Buongiorno A, O Arino, C Zehner, P Colagrande & P Goryl: ERS-2 monitors exceptional fire event in South-East Asia, *EOQ*, 56-57, Dec. 1997.

Dozier J: A method for satellite identification of surface temperature fields of subpixel resolution. *Remote Sensing of the Environment*, **11**, 221-229, 1981.

Eva H, G D'Souza & JP Malingrau: Potential of ATSR-1 data for detection of clearings within the dense humid tropical forest, *Int J of Remote Sensing*, **16**, 2071-2079, 1995.

Pereira J: A comparative evaluation of NOAA/AVHRR vegetation indices for fire scar detection and mapping in the Mediterranean-type region. *in press, IEEE Trans. Geosc. & Rem. Sens.*, 1998.

Martin Rico C: The Fuego System, personal communication at the ATSR Fire Atlas Meeting, ESA/ESRIN, 15 January 1998.

### Preliminary study on ATSR-2 pixel position for pixel-based temporal analysis.

